

is observed among their heterozygous *rde* (+) or *mut* (+) F<sub>1</sub> cross-progeny. This type of inheritance occurs only in hermaphrodites and may reflect a passive transfer of the injected material into the maternal germ line. The activities of *rde-1* and *rde-4* genes are necessary in the ensuing generation for the initiation of interference in response to this inherited material.

24. Homozygous hermaphrodites of *rde-1* and *rde-2* strains were allowed to mate with males of the same strains and then injected with *pos-1* or *mom-2* dsRNA (5 mg/ml). More than 400 F<sub>1</sub> hermaphrodites from each strain were picked (10 worms per plate) and their broods were examined for the occurrence of inviable *pos-1*-like or *mom-2*-like embryos. Similarly, 300 F<sub>2</sub> animals from these injections were ana-

lyzed. Finally, 60 F<sub>1</sub> males from each strain were mated and 300 of their F<sub>2</sub> progeny were examined for affected embryos. No *pos-1* affected embryos were observed in any generation.

25. Thirty-five *rde-1* homozygous animals generated through crosses shown in Fig. 3A were tested by feeding bacteria expressing *pos-1* dsRNA and 21 similar animals were tested by direct injections of *pos-1* dsRNA; all animals tested were resistant to *pos-1* (RNAi).

26. R. Ketting *et al.*, *Cell* **99**, 133 (1999).

27. A. Schmidt *et al.*, *Genetics* **151**, 749 (1999).

28. A. J. Hamilton and D. C. Baulcombe, *Science* **286**, 950 (1999).

29. C. E. Rocheleau *et al.*, *Cell* **90**, 707 (1997).

30. The alleles of RNAi-deficient mutants used in this study were as follows: *rde-1(ne300) unc-42*, *rde-1(ne219)*, *rde-2(ne221)*, *rde-4(ne299)*, and *mut-7(pk204)*.

31. We thank T. H. Shin, M. Soto, A. Fire, and members of our laboratory for many discussions; Y. Bei and T. Shin for help in scoring RNAi mutant embryos; G. Seydoux for the *pes-10::gfp* strain; and the anonymous reviewer for helpful suggestions. Some strains were obtained from the *C. elegans* Genetic Stock Center, which is funded by a grant from the NIH National Center for Research Support. Supported in part by a Pew scholarship to C.C.M. and by NIH grant GM58800.

20 December 1999; accepted 9 February 2000

# Single-Molecule Study of Transcriptional Pausing and Arrest by *E. coli* RNA Polymerase

R. John Davenport,<sup>1\*</sup> Gijs J. L. Wuite,<sup>2\*</sup> Robert Landick,<sup>3</sup> Carlos Bustamante<sup>1,2,4†</sup>

Using an optical-trap/flow-control video microscopy technique, we followed transcription by single molecules of *Escherichia coli* RNA polymerase in real time over long template distances. These studies reveal that RNA polymerase molecules possess different intrinsic transcription rates and different propensities to pause and stop. The data also show that reversible pausing is a kinetic intermediate between normal elongation and the arrested state. The conformational metastability of RNA polymerase revealed by this single-molecule study of transcription has direct implications for the mechanisms of gene regulation in both bacteria and eukaryotes.

Transcription elongation is a key step in the regulation of gene expression in cells. During elongation, RNA polymerase (RNAP) is known to move discontinuously, spending proportionally more time at some template positions, known as pause sites, than at others (1–3). These pauses are important for regulation and may precede other elongation events such as termination and arrest (4). Regulatory molecules in both bacteria and eukaryotes can switch RNAP to a pause- and termination-resistant form, but the chemical nature of this switch is not understood at present. Most of these dynamics have been characterized on complexes artificially halted by nucleotide starvation. These experiments indicate that during elongation, the 3' end of the RNA can be displaced from the enzymes' active site either inducing pausing or extensive backtracking along the template, leading to arrest (5–8). Evidence of

the conversion among these different states has not been obtained from molecules transcribing without interruption. To characterize these transcriptional dynamics and to establish the link between backtracking, pausing, and arrest by RNAP during continued elongation, we set out to follow directly the translocation of individual RNAP molecules along the DNA strand. This approach reveals important dynamics that are averaged out in bulk experiments. Although single-molecule experiments have already revealed several aspects of interactions between *E. coli* RNAP and DNA (9–16), single-molecule kinetics of transcriptional pausing have not been reported.

We followed transcription by single molecules of RNAP ( $n_{\text{tot}} = 87$ ) in real time, using an integrated optical-trap/flow-control (OTFC) video microscope (Fig. 1) (17). There are three main advantages to this microscope. First, translocation of RNAP and pausing events can be directly observed in real time over long template lengths [ $1.1 \pm 0.7$  kilobase pairs (kbp)], because laser radiation damage is minimized. Second, by using hydrodynamic flow forces far below the stalling force, spatial and temporal resolutions are obtained that are better than assays based on Brownian motion (12, 15, 18). Third, pausing

and other transcription events can be probed not only as a function of solution conditions, but also as a function of applied load force.

Figure 2 shows two examples of the shortening of the DNA tether between the two beads because of transcription activity by individual RNAP molecules (19, 20). Several features are immediately apparent: The rate of tether shortening is variable, RNAP sometimes pauses temporarily (Fig. 2, arrows), and the enzyme eventually stops permanently (Fig. 2, asterisk). The transcription rates are determined from the slopes of these plots and can be related to the position of the molecules on the template (Fig. 2, insets). The peak transcription rates appear in this graph as local maxima, and the temporary pauses as local minima (21).

The peak transcription rates displayed by each polymerase molecule between pauses were determined and averaged. This average peak rate varied significantly from molecule to molecule [2 to 11 bp/s for 0.2 mM nucleotide triphosphates (NTPs)]. To determine whether this variation was caused by different load forces applied to the various molecules, the mean of the average peak transcription rates for all molecules transcribing at a given force was determined and plotted against force (Fig. 3A). We found that the mean of the average peak transcription rates did not vary with force in the range of 0 to 15 pN, consistent with recent observations (14). The mean of the average peak transcription rate for all molecules ( $n = 38$ ) over the complete force range was  $7.3 \pm 3$  bp/s, and the mean of the average rates (i.e., including pauses) was  $4.3 \pm 2$  bp/s for 0.2 mM NTPs and  $14.5 \pm 4$  bp/s and  $8.0 \pm 3$  bp/s, respectively, for 1 mM NTPs. These rates are comparable to those observed under similar conditions in solution (13 to 20 bp/s for 1 mM NTPs) (12) and to rates reported for single-molecule experiments on RNAP (5 to 15 bp/s for 1 mM NTPs) (12–15). Moreover, no transcriptional activity was observed beyond 15 pN, in agreement with reported stall force measurements on RNAP under slow force modulation conditions (13, 14).

The peak transcription rates for any given RNAP molecule also varies markedly along the template (2 to 27 bp/s). These variations, how-

<sup>1</sup>Department of Molecular and Cell Biology and <sup>2</sup>Department of Physics, University of California, Berkeley, CA 94720, USA. <sup>3</sup>Department of Bacteriology, University of Wisconsin, Madison, WI 53706, USA. <sup>4</sup>Physical Biosciences Division, Lawrence Berkeley Laboratory, Berkeley, CA 94720, USA.

\*These authors contributed equally to this work. †To whom correspondence should be addressed. E-mail: carlos@alice.berkeley.edu

## REPORTS

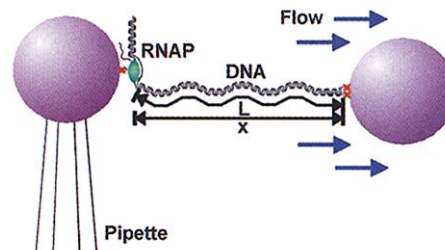
ever, were not correlated to template positions (Fig. 3B). Therefore, it is unlikely that the dispersion in average peak transcription rates among molecules (Fig. 3A, inset) arise from a heterogeneous molecular population generated during preparation. Rather, these observations suggest that transcribing RNAP molecules can switch between more competent or less competent transcription states, and that conversion from one state to another is slow (Fig. 3A, inset) (22). Similar differences in the activity of individual molecules have been reported recently for other enzymes (23–25).

Next, we determined the positions of the pauses for all RNAP molecules studied (21, 26). A plot of their distribution along the template (Fig. 4A) shows that pauses are more likely to occur at certain discrete positions than at others. We identified nine strong peaks of transcriptional pausing within alignment error (20, 27, 28) and calculated for each pause site its pausing efficiency, which is the fraction of molecules of RNAP that pause at that position, and its half-life, which is the time it takes for half of the paused molecules to escape the pause (Table 1). Comparison of the distribution of pause sites with those determined on the same template, using transcriptional gel assays, shows a reasonable agreement (Fig. 4A).

To determine whether pauses correspond to states off the main elongation pathway, we set out to establish if these pauses occur in competition with transcriptional elongation. If a paused complex is a state off the elongation pathway, not all molecules will pause at a given pause site (efficiency <100%). On the other hand, if the observed pauses correspond to states within the elongation pathway, all molecules must necessarily enter the pause state (efficiency ~100%). The pausing efficiencies we measured were <100% (Table 1, column A). Pause efficiencies, however, may be underestimated because irreversibly stopped molecules, although included in the total number of molecules, are not counted as having paused. Combining the pause and stop efficiencies at each site still does not elevate the total efficiency to 100% (Table 1, column B). The fact that pausing half-life and efficiency are uncorrelated [linear correlation coefficient  $r \approx 0.2$  (Table 1)] support the conclusion that pauses occur as states off the main elongation pathway (29). Moreover, we found a strong correlation between the inverse of the average peak transcription rate (i.e., the average time spent at each base) and pausing efficiency (Fig. 5A). This finding further supports the idea that translocation and pausing compete kinetically, as has been proposed from conventional biochemical experiments (1, 2, 8, 30, and references therein).

In addition to pausing, all RNAP molecules stopped irreversibly before reaching the end of the template (Fig. 2). As shown in Fig. 4B, RNAP molecules are more likely to stop at certain template positions than others. More-

**Fig. 1.** A stalled complex is tethered between two 2.2- $\mu\text{m}$  streptavidin-coated beads and kept in a continuous buffer flow. The transcription template consists of linearized pPIA6, a pBR322-based vector which contains the pR promoter region from bacteriophage  $\lambda$ , modified such that the first cytosine residue appears at position +71. It also contains the fragment of the  $\lambda$  genome overlapping the *cos* region from the *Cla* I site at 16121 to the *Bam* HI site at 5505. Linearized DNA was biotinylated on one end by filling in the 5' overhanging restriction site of *Bam* HI with biotinylated nucleotides. Transcription complexes were stalled at position +70 by incubating 10 nM linearized DNA template with 40 nM biotinylated RNAP in 1 $\times$  transcription buffer [50 mM tris-Cl (pH 8.0), 200 mM KCl, 10 mM MgCl<sub>2</sub>, 1 mM dithiothreitol (DTT)] for 10 min at 37°C, then adding 200 mg heparin/ml, 100  $\mu\text{M}$  adenosine triphosphate (ATP), 100  $\mu\text{M}$  guanosine triphosphate (GTP), 20  $\mu\text{M}$  uridine triphosphate (UTP), and incubating for 10 min at 25°C. Stalled complexes were diluted to a working concentration of 40 pM in 1 $\times$  transcription buffer containing 1% DTT and 0.1% NaAzide. Transcription by tethered complexes was restarted by addition of a mixture of 200  $\mu\text{M}$  or 1 mM each ATP, cytosine triphosphate (CTP), GTP, and UTP. All experiments were performed at 20°C. As a transcribing polymerase moves along the DNA, it physically pulls the two beads closer together. The separation of the beads was measured by video microscopy and used to determine the end-to-end distance and the contour length of the DNA (19, 34).



over, these positions correspond, within the alignment error of the experiment (19, 20), to positions previously identified as pause sites. This observation and the fact that molecules do not dissociate after stopping suggest that these complexes are in arrested states similar to those previously described in biochemical assays (5–7).

Because arrest occurs at or near pause sites, it is possible that these processes are related. Therefore, we investigated whether a polymer-

ase transcribing faster, and therefore more likely to resist pausing, might also be more likely to resist arrest. To investigate this possibility, we calculated the average distance between pauses for each individual RNAP molecule and plotted it versus the total distance transcribed by that

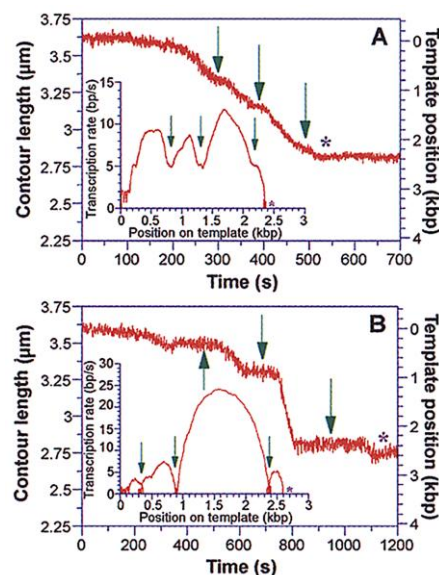


**Fig. 2.** Transcription by a single molecule of RNAP decreases the distance between the beads (34). Data was taken at tensions of 8 and 2 pN for graphs in (A) and (B), respectively. (Insets) The distance data was low pass-filtered (0.067 Hz), and a time derivative was taken to obtain the transcription rate (17). If a pause is shorter than the filtering duration, then the rate does not drop to zero. The position of the RNAP on the template during transcription is known, because all molecules are stalled at position +70 downstream of the promoter, and resumption of transcription is directly observed.

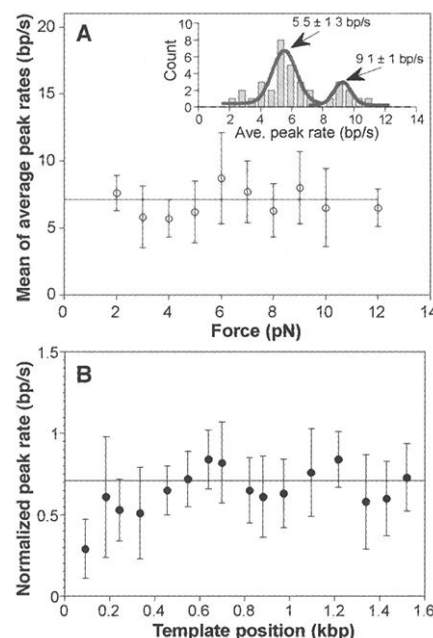


**Fig. 3.** (A) The mean of the average peak transcription rates and standard deviations were calculated at different forces. (Inset) The averaged peak rates of single enzyme molecules ( $n = 38$ ) combined in a histogram (bin size: 0.6 bp/s). The histogram shows that the enzyme can be in a slow or a fast transcription state. (B) In order to reveal a template-dependent trend in transcription rate (if any) the peak rates of each transcription run were first normalized relative to their maximum value. Hereafter, the normalized peak rates of the experiments were combined together. Finally, the template was divided in 60- to 90-bp pieces, and the normalized peak rates within these segments were averaged (each point:  $n > 5$ ).

REPORTS

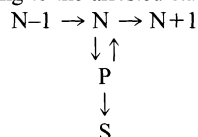
**Table 1.** At each pause site, the number of molecules which pause reversibly (P), the number of molecules which irreversibly stop (S), and the number of molecules which pass through the site without pausing (E) were counted ( $N_{\text{tot}} = 40$ ). The pausing efficiencies were determined as described in Fig. 4 (excluding S in column A). To determine if pauses are correlated, the conditional probability was determined between pausing in position  $i$  and  $i+1$ . We found that these probabilities were independent [ $P(i+1|i) = P(i+1)$ ].

Pause number	A Pause efficiency (%) $\pm 10\%$ $P/(S+P+E)$	B Pause efficiency (%) $\pm 10\%$ $(P+S)/(S+P+E)$	C Half-life (s)	D Rate at Pause site (bp/s)	E Pause efficiency (%) $\pm 15\%$ 2 to 4.5 pN	F Pause efficiency (%) $\pm 11\%$ 5 to 8.5 pN	G Pause efficiency (%) $\pm 20\%$ 9 to 15 pN
1	56	57	39	0.3	67	67	66
2	45	54	30	0.2	50	63	67
3	39	48	32	-0.1	63	58	-
4	40	50	21	0	62	55	-
5	41	54	19	-0.3	-	47	25
6	35	45	28	0.6	50	36	33
7	30	46	53	0.5	50	58	45
8	57	63	13	-0.3	80	54	62
9	39	45	12	-0.2	39	49	66

Column D shows the average transcription rates of paused RNAP enzymes at the pause sites. Each is below our rate resolution of 1 bp/s (27), indicating that RNAP enzymes indeed temporarily stops at pause sites. The pause durations for all molecules at a given pause position were combined to create a plot of the fraction of molecules still paused versus time. The half-life was extracted using an exponential fit through the resulting graph.  $(P+S)/(S+P+E)$  was also determined in three separated force regimes (columns E through G).

molecule before arrest (Fig. 5B). The distance between pause events is remarkably correlated to the total distance transcribed (Fig. 5B) (30). This behavior again suggests that some molecules in the population are indeed better than others at avoiding pauses, and that avoiding these pauses makes those molecules less likely to arrest, thus allowing them to transcribe further. The simplest kinetic mechanism by which a molecule that is better at avoiding pauses is also better at eluding arrest is one in which the

pause state is an intermediate in the kinetic pathway leading to the arrested state.



This kinetic scheme, where N is nucleotide position, P is pause, and S is stop, explains the spatial coincidence between pauses and arrests. Furthermore, such a scheme predicts a signifi-

cant correlation between the pausing half-life and arrest efficiency. This correlation is indeed found [linear correlation coefficient  $r \approx 0.75$ ,  $n = 9$  (Table 1)].

External force did not affect the combined pause and arrest efficiency  $[(P+S)/(P+S+E)]$  (Table 1). However, in the high-force regime (9

**Fig. 4.** (A) (Gray Gaussians) The positions of 241 local minima (pauses) and 51 irreversible stops (arrests) of 51 molecules were binned with 30-bp bins and normalized. Peaks taller than 0.8 were selected. All pauses within the alignment error ( $\pm 60$ -bp or  $\pm 20$  nm) (20) of these peaks were used to calculate the fraction of molecules which paused at these positions. The pauses outside the Gaussian distributions of the selected peaks were treated in a similar way using a 0.6 cutoff, followed by 0.4 and 0.2 cutoffs. Each of the peaks so obtained is displayed as a Gaussian (60-bp SD) with an surface area equal to the pause efficiency at that location. (Black line) Biochemical pausing assays were performed using the transcription reaction described above, except that 100  $\mu$ M ATP, 20  $\mu$ M GTP, 20  $\mu$ M UTP, and 1 mCi/ml [ $\alpha$ - $^{32}$ P] GTP were used to form stalled complexes. The complexes were diluted 1:10 into transcription buffer containing 200  $\mu$ M each ATP, GTP, UTP, and CTP. Aliquots (5  $\mu$ l) were taken at 30 s, 1 min, 5 min, and 10 min and quenched in 10  $\mu$ l of RNA loading buffer (95% formamide, 20 mM EDTA, 0.01% bromophenol blue, 0.01% xylene cyanol). Aliquots were electrophoresed on a 4% acrylamide gel containing 7 M urea. Bands were sized by comparison with denatured 1 kb DNA ladder and 0.16 to 2.77 kb RNA Ladder (GIBCO-BRL), quantitated using a Storm 860 phosphorImager and ImageQuant software. The resulting gel profiles were combined and plotted in the graph. The heights of the pausing intensity peaks are different for both techniques because in the gel assay they are a function of both the pause efficiency and the pause duration, whereas in the single molecule assay they represent the fraction of molecules that actually pause at a particular position. (B) Molecules that failed to reenter elongation after pausing for more than 10 min were assumed to be irreversibly stopped. Stop positions for 51 molecules were binned with 60-bp bins. The positions with highest occurrences of stops were selected. The stop efficiencies were determined in a similar fashion as the pause efficiencies (Table 1). The error in the determination of these efficiencies is  $\pm 6\%$ .

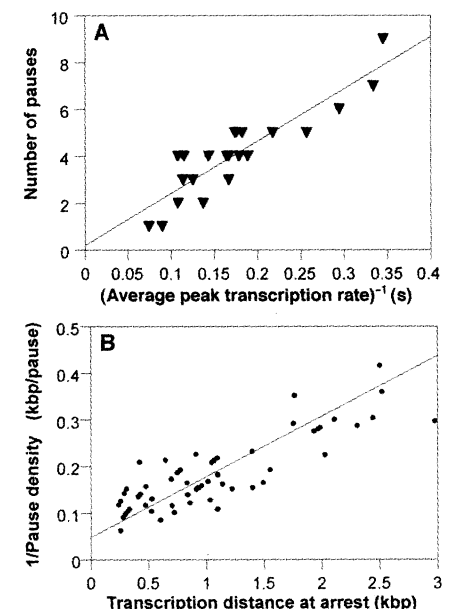
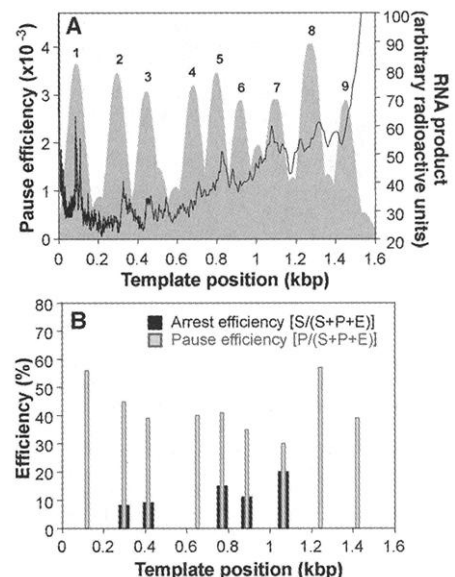


**Fig. 5.** (A) To determine the relation between the average time spent at each base position and the number of pauses, molecules which transcribed at least 1.23 kbp, a stretch of the template which includes eight identified pause site, were used. The number of pauses and the inverse of the average peak transcription rate for each of the RNAP molecules within this stretch were obtained and plotted in the graph. (B) The pause density for an individual molecule was determined as the quotient of the transcription distance and the total number of pauses for that molecule. The inverse of this number was plotted against the distance the RNAP molecule transcribed before arresting.

to 15 pN), the incidence of arrest  $[S/(S+P+E)]$  during a pause nearly tripled for most of the pause positions as compared to the low-force regime. These observations again support the branched kinetic pathway described above. As stated earlier, external force ( $<15$  pN), has a negligible effect on the rate of transcription, and accordingly, it does not affect the fraction of molecules that leave the main elongation pathway to pause. Higher external forces may, however, accelerate the rate at which molecules that are already paused can convert into the arrested state or, alternatively, decrease the rate at which these paused molecules can escape the pause to reenter elongation. Interestingly, the pause duration averaged over all pauses was insensitive to the magnitude of the applied force (up to 15 pN), indicating that the external force mainly increases the rate of conversion to the arrested state.

Landick (8, 31, 32) proposed a model in which, at every template position, the molecules can partition themselves between normal elongation and a state susceptible to pausing, arrest, and termination. According to this model, the RNA 3' end is displaced from the active site via either disrupted RNA:DNA base-pairing or some degree of slippage upon entry into a pause. Such paused complexes could vary in structure from a pretranslocated complex to a complex that has backtracked many base pairs (5, 6, 33). By using an OTFC video microscope, we have shown that a paused state is, in fact, a kinetic intermediate between forward elongation and an arrested state. Having entered a pause state, the application of external force favors the formation of an arrest state perhaps by inducing backtracking of the complex (14). Moreover, molecules appear to switch spontaneously between states that are transcriptionally more competent or less competent, becoming, respectively, more susceptible or less susceptible to pausing. It is interesting to speculate that switching among these alternative states may be the basis of yet one more level of transcriptional control and regulation.

References and Notes

1. G. A. Kassavetis and M. J. Chamberlin, *J. Biol. Chem.* **256**, 2777 (1981).
2. J. R. Levin and M. J. Chamberlin, *J. Mol. Biol.* **196**, 61 (1987).
3. D. N. Lee and R. Landick, *J. Mol. Biol.* **228**, 759 (1992).
4. T. D. Yager and P. H. von Hippel, in *Escherichia coli and Salmonella typhimurium: Cellular and Molecular Biology*, F. C. Neidhardt et al., Eds. (American Society for Microbiology, Washington, DC, 1987), pp. 1241-1275.
5. E. Nudler, A. Mustaev, E. Lukhtanov, A. Goldfarb, *Cell* **89**, 33 (1997).
6. N. Komissarova and M. Kashlev, *J. Biol. Chem.* **272**, 15329 (1997).
7. M. Palangat, T. I. Meier, R. G. Keene, R. Landick, *Mol. Cell* **1**, 1033 (1998).
8. R. Landick, *Science* **284**, 598 (1999).
9. H. Kabata et al., *Science* **262**, 1561 (1993).
10. M. Guthold et al., *Biophys. J.* **77**, 2284 (1999).
11. S. Kasas et al., *Biochemistry* **36**, 461 (1997).
12. D. A. Schafer, J. Gelles, M. P. Sheetz, R. Landick, *Nature* **352**, 444 (1991).
13. H. Yin et al., *Science* **270**, 1653 (1995).

14. M. D. Wang et al., *Science* **282**, 902 (1998).
15. H. Yin, R. Landick, J. Gelles, *Biophys. J.* **67**, 2468 (1994).
16. H. Yin et al., *Proc. Natl. Acad. Sci. U.S.A.* **96**, 13124 (1999).
17. A water immersion, high numerical aperture (NA = 1.2) objective lens with a 220- $\mu$ m working distance allows the stable trapping of a micrometer-sized sphere 100  $\mu$ m from the cover slip surface of the fluid chamber with a single-laser beam optical trap ( $\lambda = 835$  nm). This design makes it possible to introduce a micropipette in the chamber to hold a bead by suction. The bead in the trap and the bead on the pipette function as easily exchangeable surfaces between which RNAP molecules can be attached. A computer-controlled flow system is used to exchange the liquid in the fluid chamber and to establish a flow rate with high precision. The flow can be used to exert force on the beads, whose displacements are then measured by video microscopy (at 10 Hz in real time). The instrument is highly automated to maximize experimental throughput. Individual stalled elongation complexes were assembled between two beads, one held in a laser trap and the other held on a micropipette. After assembly, the trapped bead was released from the trap to avoid laser damage to the transcription complex. The complex was then extended by drag applied on the bead. The flow could be increased or decreased to vary the hydrodynamic drag force on the tethered bead, and therefore, the load force acting on the polymerase. Upon addition of NTPs, we followed the resumption of transcription by the shortening of the DNA tether between the beads. A movie of transcription by a single molecule of RNAP can be viewed at <http://alice.berkeley.edu/RNAP>
18. The position resolution of a tethered bead is  $\sim 21$  base pairs (bp) ( $\sim 7$  nm). This position resolution is determined by the rms displacement due to brownian motion after averaging over 0.033 s ( $\sim 4$  nm) added to the error of the bead centroid determination ( $\sim 3$  nm) (34). The tethered particle motion method has a resolution of 400 bp using a DNA fragment 10 times shorter and averaging over 0.27 s (15).
19. The end-to-end distance of the DNA ( $x$ ) is obtained by subtracting the radii of the beads ( $B_{corr}$ ) from the center-to-center bead distance ( $x_m$ ). The applied force ( $F$ ), created by hydrodynamic drag by the buffer flow on the bead, was calibrated to the flow speed. The value of  $x$  depends on the contour length ( $L$ ) of the tethered DNA (i.e., on the position of the polymerase along the DNA) and on the tension along the molecule. For forces greater than 2 to 3 pN,  $L$  is related to  $x$  by the relationship [T. Odijk, *Macromolecules* **28**, 7016 (1995)]

$$L = \frac{x}{\left(1 + \frac{F}{S}\right) \left(1 \pm \sqrt{\frac{k_B T}{4PF}}\right)}$$

where  $S$  and  $P$  are the stretch modulus and the persistence length of double-stranded DNA, respectively,  $k_B$  is the Boltzmann constant, and  $T$  is the absolute temperature.

20. The calculated contour length may differ from the real contour length depending on the point of attachment of the complex on the pipette bead. A correction factor ( $B_{corr} = x_m - x$ ) can be calculated for each data set, using  $x_m$  before transcription begins and  $x$  for a 3.61- $\mu$ m DNA molecule. The error in  $x$  depends on the force uncertainty ( $\sim 10\%$ ), and  $x_m$  can be obtained accurately by averaging the signal for  $\sim 100$  s. This results in an error in  $B_{corr}$  of  $\sim 10$  nm at 5 pN. Within one data set, the pause positions are known with a  $\sim 10$ -nm resolution (34). However, when the pause positions of all molecules are combined, the error in  $B_{corr}$  introduces an alignment error of the different data sets resulting in  $\sim 20$  nm total error.
21. We applied a computer algorithm to determine the positions of the local minima and maxima. Local extrema were scored when the second time derivative of the position, averaged over 10 s, were between 0.1 and 0 bp/s<sup>2</sup>. Brownian motion limits the resolution of rate determination to  $\pm 1$  bp/s (2 SD) as determined from the distribution of rate fluctuation of beads tethered to nontranscribing polymerases. The quantitative criterion used to score whether an enzyme has paused is the following. A pause is scored if the rate of transcription at that location is below the limit of rate resolution (1

bp/s). The rate at the local rate minimum was determined by fitting a line to the position versus time data for the duration of the pause (26). This analysis made it possible to distinguish between pauses and locations in which the enzyme had simply slowed down but had not paused.

22. Analysis of the enzyme population displaying this bimodal distribution reveals that  $\sim 75\%$  of the molecules exist in a slow state for most of the time that they transcribe (these are often RNAP enzymes which transcribed for shorter times). The fast-transcribing enzymes, on the other hand, were more prone to change rate to become slower transcribers. The different heights of the peaks in the bimodal distribution are likely to arise from this difference in switch behavior between the two populations. Most RNAP enzymes that transcribe longer distances (and times) undergo one, or sometimes more, rate changes. Changes in peak rate up to 18 bp/s have been observed for some molecules. The most frequent changes in peak rate are  $\pm 2$  bp/s ( $n = 18$ ), followed by changes of  $\pm 4$  to 5 bp/s ( $n = 11$ ). Changes smaller than  $\pm 1$  bp/s are indistinguishable from Brownian motion (27). The most frequent rate changes are sufficient to allow a molecule to jump from the slow to the fast transcribing state in the histogram in Fig. 3A, and vice versa.
23. H. P. Lu, L. Xun, X. S. Xie, *Science* **282**, 1877 (1998).
24. Q. Xue and E. Yeung, *Nature* **373**, 681 (1995).
25. G. J. L. Waite, S. B. Smith, M. Young, D. Keller, C. Bustamante, *Nature* **404**, 103 (2000).
26. The pause duration is taken as the time it takes an enzyme to move from a position 30 bp before the pause to another location 30 bp after the pause (twice the spatial resolution).
27. The precise template position of a pause cannot be determined at the present resolution of the experiment (20, 34). However, the average spacing between detected pauses ( $\sim 200$  bp) is  $\sim 3.5$  times the spatial uncertainty in their position. Some of the pausing events detected may, nonetheless, correspond to several closely-lying pauses. On average, molecules translocate for about 75 s before pausing. This figure is five times longer than the filter frequency used on the data. Thus, the majority of pauses are detected.
28. The same nine peaks were present when similar histograms were generated from 23 data sets picked randomly from the complete data set.
29. If pausing corresponds to a state on the same kinetic pathway as normal elongation, then the half-life and "apparent efficiency" at each pause site would be correlated to one another, since both depend on the forward rate constant for the next template position. In other words, if a site had a relatively long half-life, this long residence time would make it more likely that the pause will be scored, thus introducing a correlation between the half-life and the apparent efficiency.
30. If one assumes that all molecules are identical, i.e., that all molecules have the same chance to pause or arrest at a given branch leading to these states, and that pauses are approximately evenly spaced, the distance between pauses should be independent of the distance transcribed by the molecule before arrest.
31. R. Landick, *Cell* **88**, 741 (1997).
32. I. Artsimovitch and R. Landick, *Genes Dev.* **12**, 3110 (1998).
33. N. Komissarova and M. Kashlev, *Proc. Natl. Acad. Sci. U.S.A.* **94**, 1755 (1997).
34. The bead position is determined by averaging the positions of all the pixels inside the circular black edge of the bead image (the resolution of this procedure is  $\sim 3$  nm). The experimental uncertainty in the determination of the center-to-center bead distance for a 2.2- $\mu$ m diameter bead held at the end of a 3.5- $\mu$ m-long DNA molecule extended by a drag force of 5.5 pN is 9.8 nm (i.e.,  $\sim 4$  nm of rms displacement due to Brownian motion plus twice the error in the bead centroid determination, or  $\sim 6$  nm).
35. Supported by NIH grant GM-32543 and NSF grants MBC 9118482 and DBI 9732140 to C.B. and by NIH grant GM-38660 to R.L. The authors thank C. Rivetti, D. Erie, and F. Stahl for providing tools for the construction of the DNA template and S. B. Smith, M. Hegner, Z. Bryant, and M. Young for many helpful discussions.

20 December 1999; accepted 9 February 2000